Cellulose nanofibril film as a piezoelectric sensor material

Satu Rajala[1‡], Tuomo Siponkoski[2], Essi Sarlin[3], Marja Mettänen[1], Maija Vuoriluoto[4], Arno Pammo[1], Jari Juuti[2], Orlando J. Rojas[4], Sami Franssila[5] and Sampo Tuukkanen[1‡]*

[1] Department of Automation Science and Engineering, Tampere University of Technology, P.O. Box 692, FI-33101 Tampere, Finland, satu.rajala@tut.fi, marja.mettanen@tut.fi, arno.pammo@tut.fi, sampo.tuukkanen@tut.fi,

[2] Microelectronics Research Unit, Faculty of Information Technology and Electrical Engineering, University of Oulu, P.O. Box 4500, FIN-90014 Oulu, Finland, tuomo.siponkoski@oulu.fi, jari.juuti@oulu.fi

[3] Department of Materials Science, Tampere University of Technology, P.O. Box 692, FI-33101 Tampere, Finland, essi.sarlin@tut.fi

[4] Department of Forest Products Technology, School of Chemical Technology, Aalto University, P.O. Box 16300, FI-00076 Aalto, Finland, maija.vuoriluoto@aalto.fi, orlando.rojas@aalto.fi

[5] Department of Materials Science and Engineering, School of Chemical Technology, Aalto University, P.O. Box 11000, FI-00076 Aalto, Espoo, Finland, sami.franssila@aalto.fi

Keywords: Cellulose nanofibrils; Piezoelectric sensors; Image based analysis; Sensitivity measurement.

Abstract

Self-standing 45-μm-thick films of native cellulose nanofibrils (CNF) were synthesized and characterized. The surface and the microstructure of the films were evaluated with image based analysis and scanning electron microscopy (SEM). Dielectric properties of the films were measured obtaining relative permittivity of 3.47 and 3.38 and loss tangent tan δ of 0.011 and 0.071 at 1 kHz and 9.97 GHz, respectively. The films were used as functional sensing layers in piezoelectric sensors for which sensitivities from 4.7 to 6.4 pC/N were measured in ambient conditions. This piezoelectric response is expected to increase remarkably after polarization of crystalline cellulose regions in the film. The CNF sensor characteristics were evaluated and compared with a reference piezoelectric polymer (polyvinylidenefluoride, PVDF). Overall, the results suggest that nanocellulose is a suitable precursor for disposable piezoelectric sensors with potential applications in fields of electronics, sensors and biomedical diagnostics.

1. Introduction

Cellulosic nanofibrils and nanocrystals[1], referred to as nanocelluloses, are interesting renewable bio-based nanomaterials with potential applications in different fields. The nanoscale dimensions and strong ability to form entangled porous networks make nanocelluloses suitable materials for fabrication of light-weight membranes, films, and nanopapers, all of which can be

processed in aqueous media. The use of solution-processable functional materials allows the low cost and high throughput manufacturing of devices for electronics[2,3], sensors[4] or optics[5]. Furthermore, when using nanocellulose in combination with solution-processable carbon based nanomaterials, such as carbon nanotubes or graphene, flexible and disposable supercapacitors can be prepared[6–8].

The piezoelectricity of wood has been known for decades[9,10]. A classical definition of piezoelectricity is the change of electrical polarization in a material in response to mechanical stress[11]. This phenomenon is more pronounced in crystalline nanoscale materials, such as cellulose nanocrystals (CNC)[12,13]. However, the topic has been covered in the scientific literature to a very limited extent and only few recent studies report experimental evidence of CNC piezoelectricity[12,14]. Herein, Frka-Petesic et al. reported recently about the experimental evidence of giant permanent electric-dipole moment in cellulose nanocrystals[14]. Compared to CNC, the higher aspect-ratio cellulose nanofibrils (CNF), containing both crystalline (cellulose I^1) and amorphous phases, can offer more versatile options as far as the synthesis of self-standing films and nanopapers is profitable. Despite the principally randomly aligned crystalline regions in CNF, their films are expected to show some level of piezoelectric behavior due to the film fabrication process driven alignment. To our knowledge, piezoelectric measurements of CNF films have not been attempted before the authors contribution[15,16].

In this study, CNF films were fabricated and characterized through imaging, density and dielectric measurements and electromechanical sensitivity measurements. The microstructure of the films was studied using scanning electron microscopy (SEM). Also, the surface of the films

was evaluated through measurements based on optical images. The films were used as functional materials in piezoelectric sensors and their sensitivity was measured by using a custom-built setup. The sensors were excited with a shaker that delivered a sinusoidal input force and the charge generated by the sensors was measured. The sensitivity is defined here as the charge generated by the sensor divided by the force applied to excite the sensor. Finally, the sensor characteristics including nonlinearity and hysteresis were measured and compared with a reference piezoelectric polymer film (polyvinylidenefluoride, PVDF).

2. Materials and methods

2.1 Nanocellulose Piezoelectricity

The compression of a piezoelectric film by an external force causes charge separation in the film generating a noticeable voltage between two electrodes. The piezoelectric coefficient d_{mn} is related to the charge density generated under a certain applied stress. A third-rank tensor of piezoelectric coefficients d_{mn} is expressed in terms of 3×6 matrix, where $m = 1, 2, 3$ refers to the electrical axis and $n = 1, 2, \ldots, 6$ to the mechanical axis[11]. The main axes 1, 2 and 3 correspond to length, width and thickness, whereas the shear around these axes is represented by 4, 5 and 6.

The piezoelectric tensor d_{mn} can be derived from the symmetry of a cellulose crystal lattice, formed by unit cells of cellulose molecules $([C_6H_{10}O_5]_n)$[10]. Cellulose belongs to a monoclinic symmetry with space group of $C_2 \parallel x_3$ having a following piezoelectric tensor:

$$d_{mn} = \begin{pmatrix} 0 & 0 & 0 & d_{14} & d_{15} & 0 \\ 0 & 0 & 0 & d_{24} & d_{25} & 0 \\ d_{31} & d_{32} & d_{33} & 0 & 0 & d_{36} \end{pmatrix}. \quad (1)$$

This tensor is valid for a single cellulose crystal. However, for a film with randomly aligned crystals (such as CNF film studied in this work), the overall piezoelectric response of the film is a combination of different coefficients. For example, in the case of wood, arrangement of fibers and accompanied cellulose crystals have been shown to exhibit greatly reduced effective piezoelectric tensor:

$$d_{mn} = \begin{pmatrix} 0 & 0 & 0 & d_{14} & 0 & 0 \\ 0 & 0 & 0 & 0 & d_{25} & 0 \\ 0 & 0 & 0 & 0 & 0 & 0 \end{pmatrix}, \quad (2)$$

where $d_{14} = -d_{25}$ [9,10].

2.2. CNF film fabrication

Figure 1 describes schematically the deconstruction of nanocellulose from wood cellulose fibers[1]. In this work, an industrial-grade bleached sulphite birch fibers suspended in water were processed through a Masuko grinder using three consecutive passes and further homogenized using six passes at 2000 bar pressure by using a M110P microfluidizer (Microfluidics Corp., Newton, MA, USA) equipped with 200 and 100 µm chambers. The resulting CNF material is composed of crystalline (cellulose I[1]) and amorphous domains. When dispersed in the aqueous medium, CNF was highly viscous and it can be classified as a hydrogel[17]. Films based on CNF were fabricated by pressure filtering (15-30 min) followed by pressing and drying in a hot-press

at 100 °C for 2 h (described previously in more details[18]). An example of the resulting self-standing CNF films is presented in the Figure 2a.

2.3. CNF film characterization

The CNF film was characterized by Scanning Electron Microscopy (SEM, Zeiss ULTRAplus). Cross-sectional images were obtained by breaking the CNF film under liquid nitrogen and by gluing the film to sample holders with conductive carbon cement. The samples were coated with a thin carbon layer to provide electrical conductivity prior to the SEM imaging. Energy Dispersive X-ray Spectroscopy (EDS, INCA Energy 350 with INCAx-act detector) was used to ensure the purity of the CNF film. The apparent film density was calculated for a 5 cm x 8 cm piece of CNF film by assuming an even film thickness obtained from the SEM analysis and mass weighted by a microbalance.

The surface structure of the CNF film was also examined through photometric stereo imaging and subsequent image analysis. Photometric stereo[19] is a widely used technique in computer graphics for surface analysis and reconstruction[20], and it has also been successfully applied in small-scale surface topography measurement, e.g., in paper industry[21] and dermatology[22]. In photometric stereo setup, the translucent CNF sample lied still on top of a flat black sheet of cardboard while it was imaged with a camera from the top. Four images were taken from the sample with different, but precisely known, illumination directions, using blue LEDs whose dominant wavelength was 460 nm. The surface orientation (i.e., gradients) at each pixel was estimated from the photographs; see Ref. [19] for details. The surface topography map was then

reconstructed from the gradient fields by integration[23]. The photographs were captured using a digital systems camera (Canon EOS 550D) and a magnifying macro lens (Canon MP-E 65 mm). With a slight magnification (1.3:1), a pixel size of 3.27 μm x 3.27 μm on an image area of approximately 17 mm x 11 mm was achieved.

The dielectric properties of the CNF film were measured at 100 Hz to 1 MHz by using a LCR meter (precision LCR meter 4284A, Keysight Technologies, USA). In order to increase reliability of the measurement a stack of two films (total thickness of 96 μm) was measured instead of a single 45 μm thick film. The sample was compressed gently between two external electrodes of diameters 25 and 17.5 mm in a custom made measurement setup. The holder of smaller electrode was made from soft rubber, covered with a conductive layer. This enabled the sample to align better between the electrodes and improved applying of small pressures for the sample to avoid deformation. To characterize dielectric properties also at higher frequencies, the CNF film was measured at 9.97 GHz using a Split Post Dielectric Resonator (QWED, Warsaw, Poland). This technique enables measurement without electrodes. Prior to both dielectric measurements the films were hold 60 min at 100 °C to minimize the effect of air moisture in the measurement results. Furthermore, a ferroelectric tester (Precision LC, Radiant technologies, USA) was used to measure the ferroelectric hysteresis characteristics of the CNF film up to 50 V/μm electric field using 10 Hz frequency.

2.4. CNF and PVDF sensor assembly

Electrodes for the CNF sensors were fabricated on polyethylene terephthalate (PET, Melinex ST506) substrate by e-beam evaporation (Varian vacuum evaporator). Electrodes were formed by evaporating 100 nm thick copper (Cu) layer through a laser-cut stencil shadow mask.

The preparation of piezoelectric CNF sensors is described in Figure 2. Before the sensor assembly, the CNF film shown in Figure 2a was cut into round shape pieces with a diameter slightly larger than that of the electrodes, thus to avoid electrical breakdown over the edges. The structure of the sensors is presented schematically in Figure 2b,c. The CNF pieces were then sandwiched between two electrodes and fixed together from outside of the electrode perimeter using a sticker film (2 way glue, manufactured by Kuretake Co.). A photograph of a fabricated sensor is presented in Figure 2d. The total thickness of the assembled sensor was about 300 μm, measured with a micrometer screw.

In total, four CNF sensors with electrode diameter of 15 mm were assembled and measured in this work. In addition, one larger CNF sensor (with electrode diameter of 20 mm) was fabricated and compared to a reference polyvinylidenefluoride (PVDF) sensor, assembled with the same method as the CNF sensors. A larger electrode area was used to study the sensitivity distribution over the sensor surface. PVDF is a piezoelectric polymer material that is widely used in versatile sensor applications, and thus, it was chosen here as a reference. For instance, the PVDF material is used in mechanical (e.g. pressure, acceleration, vibration and tactile sensors etc.), acoustics and IR sensors[24]. Application areas also include energy conversion[25] and medical measurements[26–28]. An unmetallized, 28 μm thick PVDF film manufactured by Measurement Specialties Inc. (Hampton, USA) was used in this study[29].

2.5. Piezoelectric sensitivity measurements

A Brüel & Kjaer Mini-Shaker Type 4810 generating a dynamic excitation force was used in the sensor sensitivity measurements. A sinusoidal input for the shaker was provided with a Tektronix AFG3101 function generator. A commercial high sensitivity dynamic force sensor (PCB Piezotronics, model 209C02) was used as a reference sensor for the dynamic excitation force. A load cell (Measurement Specialties Inc., model ELFS-T3E-20L) was used as reference sensor to measure the static force between the sample and shaker's piston (diameter 4 mm). A pre-compression, which produces the static force, is needed to keep the sample in place and to prevent the piston from jumping off the surface during the measurement. Figure 3 shows in detail the sensor sensitivity measurement setup. The same measurement principle has been previously used to evaluate the sensor sensitivity of piezoelectric polymer film (PVDF)[26–28,30–33].

The sensor sensitivity measured in this study is closely related to the longitudinal piezoelectric coefficient d_{33}. The longitudinal d_{33} coefficient describes the electric polarization generated in the same direction as the stress is applied[34]. Thus, in the measurement of the sensor sensitivity, the electrodes were located on the top and the bottom of the sensor material and the film was excited with a dynamic force in the Z or thickness direction. The sensitivity is defined here as the charge generated by the sensor divided by the normal force used to excite the sensor. The unit of sensitivity is thus C/N.

To measure the sensor sensitivity of the four CNF sensors (diameter 15 mm) in the thickness direction, the sensor was placed horizontally on the metal plate, see Figure 3. The charge developed by the sensor was measured with a custom-made combination of a charge amplifier and a 16-bit AD-converter. The connection to the AD-converter from the sensor was provided via coaxial wires and crimp connectors (Nicomatic Crimpflex). The AD-converter also had additional channels for sampling the voltage signals from the reference sensors. The measured data was processed to solve the sensitivity of the sensor to the force. Since the excitation force was sinusoidal, the sensitivity was calculated simply by dividing the amplitudes of the respective signals. Possible baseline drift in the signals was removed with high-pass filtering before the sinusoidal amplitudes were solved by fitting sinusoidal waveforms to the signals as described in the IEEE Standard for Digitizing Waveform Recorders (IEEE Std 1241).

A static force of approximately 3 N was applied. The sensor was excited with sinusoidal 2 Hz input signal of an approximate force of 1.4 N (peak-to-peak). The excitation was applied in the middle of the sensor. The measurement was repeated three times; between the measurements the static force was relieved and the sensor was re-positioned on the metal plate for a new measurement. The same measurements were conducted from both sides of the sensor, resulting in a total of six excitation rounds per sensor.

2.6. Measurement of sensor characteristics

In addition to the piezoelectric sensitivity measurements described in the previous Section, more comprehensive measurements were performed on the CNF sensor with the electrode

diameter of 20 mm. The similar measurements were also carried out with the reference PVDF sensor. First, the sensitivity distribution over the sensor surface was measured. The CNF and PVDF sensors were excited by applying force to nine different locations on the sensor area, one at a time (see Figure 8a). The same positions were excited from both sides of the sensor, resulting in a total of 18 excitation rounds per sensor.

Next, the charge developed by the CNF and PVDF sensors was measured as a function of dynamic excitation force to determine the nonlinearity of the sensor. The amplitude of the dynamic excitation force was altered from approximately 0.1 N to 5 N (peak-to-peak) with a frequency of 2 Hz. Finally, the hysteresis error for the sensors was determined. The sensor hysteresis error is defined as the deviation of the sensor's output at a specified point of the input signal when this point is approached from opposite directions[35]. Here the sensor hysteresis curve was determined by measuring the generated charge as a function of dynamic excitation force, first by increasing the force between the excitation rounds (duration about 10 seconds) and then by decreasing it. At each excitation round, no fatigue in sensor signals was observed during the excitation. The excitation force range was approximately 0.7-2.8 N (peak-to-peak) with a frequency of 2 Hz.

3. Results

3.1. CNF film characterization

Cross-sectional and plane view micrographs (SEM) of a CNF film are shown in Figure 4. The cross-section of the film (Figure 4a) reveals a layered, porous structure with an average thickness of 45 ± 3 μm. The film structure is similar to those obtained in a previous study[18]. The surface view of the film (Figure 4b) shows the random orientation of nanofibrils. No traces of defects or possible contaminants were found. The density of the CNF film was estimated to be 1.38 g/cm^3, based on measurement of film dimensions and weight measured in ambient air.

The photometric stereo images and the reconstructed surface topography map reveal a prominent streaky structure on the surface of the CNF film. Figure 5a illustrates the surface topography map, showing the typical cloudy and random appearance of webs formed from fiber suspensions. The close-up (Figure 5b,c) clearly shows the streaky pattern, presumably produced by the filter mesh on top of which the CNF film was fabricated. The distance between the diagonal streaks on the surface is approximately 140 μm, and the finer regular structure seen on each streak corresponds to the distances between the wires of the mesh, approximately 48 μm. The streaky pattern is clearly visible on both sides of the CNF film. 2D spectrum analysis of the photometric stereo based surface topography from an area of several square millimeters also confirmed the SEM-based finding that the cellulose constituents in the film are randomly oriented in the plane of the film.

The calculated relative permittivity and dielectric loss tangent values for the CNF film obtained from the LCR measurements are presented as a function of measurement frequency in Figure 6. The error bars show the approximated 2 % error for capacitance values in measurements. Obtained relative permittivity of CNF film was about 3.47 and dielectric loss (tan

δ) about 0.011 at a 1 kHz frequency. The capacitance of CNF film varied from 78 pF to 73 pF at 100 Hz to 1 MHz, respectively. The average relative permittivity and dielectric losses were 3.38 and 0.071, respectively, measured with SPDR with nominal frequency of 9.97 GHz.

The results of ferroelectric hysteresis measurements are shown in the Figure 7. The capacitance or linear component in the polarization data is dominant in the measurements at electric fields from 5 to 15 V/μm, thus showing that CNF film has no significant ferroelectric hysteresis at low or moderate electric fields (Figure 7a). However, between 40 to 50 V/μm electric fields (Figure 7b) nonlinear behavior is detected. This suggests that the film has some level of ferroelectric properties at high electric fields, but remanent polarization at 50 V/μm field is still small (0.15 μC/cm²).

3.2. Sensor sensitivity and characteristics

The operation of four nominally identical CNF sensors with diameter of 15 mm was evaluated with sensitivity measurements (Table 1). The values are presented as mean sensitivities ± standard deviations for each sensor side. The average sensitivity value for the four CNF sensors was (5.7 ± 1.2) pC/N.

The more thorough sensor characteristics measurements were performed for one CNF sensor and one PVDF reference. Figure 8a shows the excitation positions for the sensor sensitivity distribution measurement. Both sensor samples had electrodes of 20 mm in diameter while the shaker's piston was 4 mm in diameter, as illustrated in Figure 8a. In Figure 8b, the CNF and

PVDF sensor sensitivities as a function of the excitation position are shown. The sensitivity over the sensor the surface was found to be almost constant. The average sensitivity for the CNF sensor was found to be 4.7 ± 0.9 pC/N, while that of the reference PVDF sensor was 27.5 ± 2.6 pC/N.

The nonlinearity is defined as the maximum deviation of a real transfer function from a linear correlation[35]. Here the nonlinearity was determined by fitting a first degree polynomial via least-squares minimization (Matlab function polyfit). Figure 9 shows the charge generated by the CNF and PVDF sensors as a function of the dynamic excitation force. The fitted polynomials for the sensors are shown with a blue dashed line (PVDF 34.01x-9.66) and red solid line (CNF 6.51x-1.23). Instead of the maximum deviation from the linear correlation, the nonlinearity is presented here as the mean ± standard deviation of data point deviations from the fitted polynomial. For the reference PVDF sensor the nonlinearity was found to be 6.47 ± 3.76 pC and for the CNF sensor 0.86 ± 0.48 pC.

Figure 10 shows the sensor hysteresis measurement results. The measurements made by increasing the dynamic excitation force are marked with solid line and circles and the measurements made by decreasing the force with dashed line and crosses. For the reference PVDF sensor the maximum difference between the increasing and decreasing measurements was 0.93 pC and for the CNF sensor 0.92 pC.

4. Discussion

The cellulose nanofibril (CNF) films were fabricated and characterized through SEM imaging, measurements based on optical images and density measurements. The SEM images revealed a layered, porous structure. The structure of the CNF film resembles the structure of an electret material, ElectroMechanical Film (EMFi), used in sensor applications[36,37]. The surface topography of the CNF film is dominated by streaks, approximately 140 μm apart from each other, apparently reproduced from the formation fabric mesh[18]. Apart from the mesh-induced pattern, the surface of the film is fairly smooth and the fibrous structure has random orientation. The density of the CNF film was found to be 1.38 g/cm^3 which is similar to earlier study where similar films were prepared[18]. In comparison, the densities of the PVDF and EMFi sensor materials are 1.78 g/cm^3 [29] and 0.33 g/cm^3 [36], respectively. Since the CNF film has a porous structure, it is reasonable that the density of the CNF film is slightly lower that of the PVDF film. On the other hand, the EMFi film has much lower density due to the gas filled voids separated by polypropylene layers, formed during the film manufacturing process.

The CNF film permittivity was obtained from both LCR and resonator measurements and they match very well, giving a relative permittivity of about 3.4. This is close to values of dielectric polymers such as polyimide and polytetrafluoroethylene in general and since organic materials are known to have low relative permittivity, the results are considered to be reasonable[38]. The change in relative permittivity as a function of frequency was clearly seen from the LCR measurement. At the same time, dielectric losses are increasing rapidly from 10 kHz onward accompanied with steeper declining of relative permittivity which is typical indication of relaxation mechanism taking place (Figure 6). However, the change of relative permittivity was quite small, around 7 % from 100 Hz to 1 MHz, and it was at similar level as obtained at ~10

GHz, suggesting that only minor level of dielectric relaxation phenomena is occurring due Maxwell-Wagner-Sillars (MWS) type of the polarization[39]. Such polarization takes place typically at acoustic frequencies and is associated with e.g. immobilized free charges on the interfaces of different media having contrast in conductivity and permittivity. In the case of EMFi, charges are designedly introduced into the gas filled voids separated by polypropylene layers while in this case they can be byproduct of the manufacturing process, yet having effectively similar function as in EMFi. Since the sensor sensitivity measurement was carried out at low frequencies, possible influence of MWS polarization cannot be excluded at this point. Therefore, actual mechanism behind the measured results remains still unclear, and is out of scope of this paper, but can be concluded utilizing e.g. higher frequency measurements as the dielectric relaxation expands over wider frequency spectrum than MWS relaxation.

In addition, it should be pointed out that the used external electrodes pushed against the surfaces of the sample may cause errors in dielectric and ferroelectric measurements. Any porosity between the electrodes and the sample in general decreases the coupling of the electric field and measured capacitance. The surface contact is also making it difficult to distinguish which losses are from material or due to contact. Therefore, using of two different dielectric measurements, with and without electrodes, reasonable conclusions could be drawn to avoid misinterpretation.

In the ferroelectric hysteresis measurement it was noticed that CNF film can withstand quite high electric fields even though it has porous microstructure. Small ferroelectric effect could be found with electric field above ~40 V/μm. It is commonly known that organic ferroelectric

materials have usually much higher coercive field than similar inorganic materials[40]. It should be noted that the above mentioned issue with electrode contacts may hinder also ferroelectric results. With respect to the obtained results it seems that nanocellulose is acting like incipient organic ferroelectric material when very high electric field is present[40]. In such case the observed piezoelectric effect in CNF is then resulting from the permanent dipole moment of CNCs with some level of orientation due to the fabrication process of the film in contrast to earlier mentioned observations with individual CNC crystals[12,14].

The piezoelectric sensors were fabricated from the 45 μm-thick CNF film and copper electrodes evaporated on a PET substrate. The sensitivity of the fabricated sensors was measured using a dedicated measurement setup. All five (four of 15 mm and one of 20 mm electrode diameter) prepared piezoelectric CNF sensors showed similar sensor sensitivity values, with sensitivity averages from 4.7 to 6.4 pC/N. These results suggest that the nanofibrils are homogeneously distributed inside the film and the sensitivity values are reliable. Both the CNF sensor and the PVDF reference sensor were found to be rather linear inside the used measurement range. The sensor hysteresis of the CNF sensors was found to be larger than that of the PVDF sensor. However, the hysteresis was negligible for both types of sensors.

In 2000 Fukada concluded, that a shear piezoelectric coefficient d_{14} for wood cellulose is as low as -0.1 pC/N[41], which does not suggest high applicability of cellulose as piezoelectric sensor material. However, the case is different with the extracted nanocrystals and nanofibrils. There are recent experimental evidences that the orientation of CNC crystals has a significant effect on the overall piezoelectric response[12], and that CNC has a permanent dipole momentum[14]. It was also

suggested that regenerated CNC (cellulose II) has the apparent piezoelectric coefficient on the range 35-60 pC/N[13]. One should point out that the CNF film studied in this work was not optimized as a piezoelectric material and was not polarized or oriented purposely. However, the CNF film fabrication method, such as filtering and hot-pressing, may have caused some alignment of the cellulose nanofibrils inside the thick film. The sensor sensitivity obtained for the CNF film in this work is expected to significantly increase by intentional material design aiming at optimal alignment of CNC dipoles. The poling procedure, in general, consists of applying an electric field on a processed film for a certain period of time in order to generate piezoelectric properties. The poling (or other type orientation) of the CNF film should lead to the polarization of the crystalline CNC regions inside the CNF film, further leading to a remarkable increase of piezoelectric effect due to the large piezoelectric coefficient of the crystalline components[12,14]. In comparison, a sensitivity of about 27.5 pC/N was obtained here for a sensor made from a polarized 28-μm-thick PVDF film[29]. This is about four times larger than the sensor sensitivity of the CNF film measured in this work. The initial results of orientation of water-processed CNF-films, using DC voltage, suggest the potential of remarkably higher sensitivity values[16]. However, polarization of dry film is difficult due to the entangled and stiff structure of the film and thus, further fabrication process development is required in order to increase the CNF film sensitivity.

The sensor structure composing of the CNF films sandwiched between the copper electrodes on PET may affect the measured sensitivity values: the contact between the actual sensing material and the electrode is not as good as in the case of electrodes processed directly on the

sensing material. In comparison, less variation in sensitivity values were observed when electrodes were either printed or evaporated directly on PVDF film[32,33].

To conclude, functional piezoelectric sensor elements were fabricated from CNF film and subsequently their piezoelectric sensitivity was measured. Also, a principal material characterization for CNF film was done using optical and dielectric, ferroelectric and electromechanical measurements. The obtained results in this study suggest that nanocellulose film is a suitable sensor material for applications in fields such as sensors, electronics and biomedical diagnostics.

FIGURES

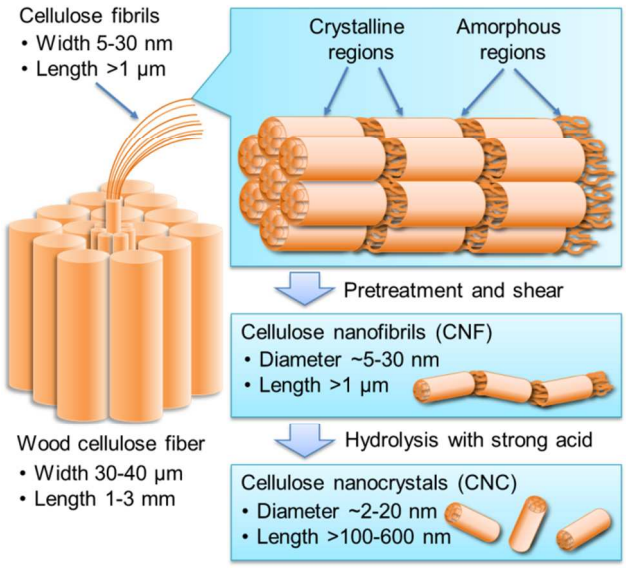

Figure 1. Schematic view of nanocellulose fabrication from wood cellulose fibers. The cellulose fibers are first deconstructed into microfibrils and after various processing steps into cellulose

nanofibrils (CNF). Cellulose nanocrystals (CNC) can be further obtained by using acid hydrolysis. For more details see reference[1].

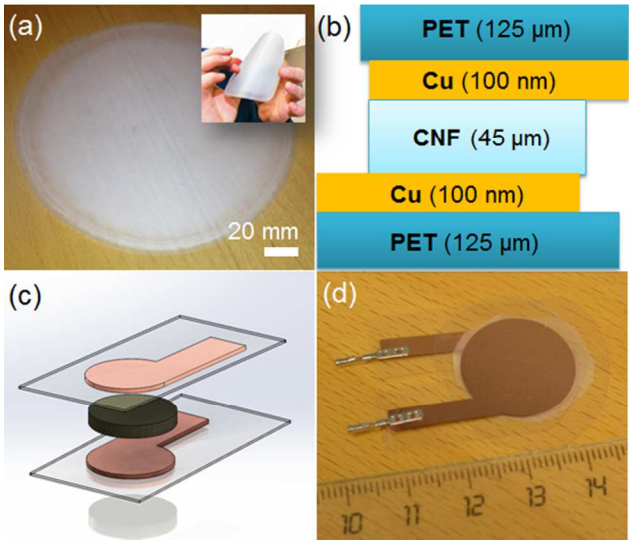

Figure 2. (a) A photograph of the fabricated self-standing CNF film. An insert image presents the bending robustness of the film. (b,c) A schematic side-view of the piezoelectric sensor structure, (d) a photograph of assembled sensor.

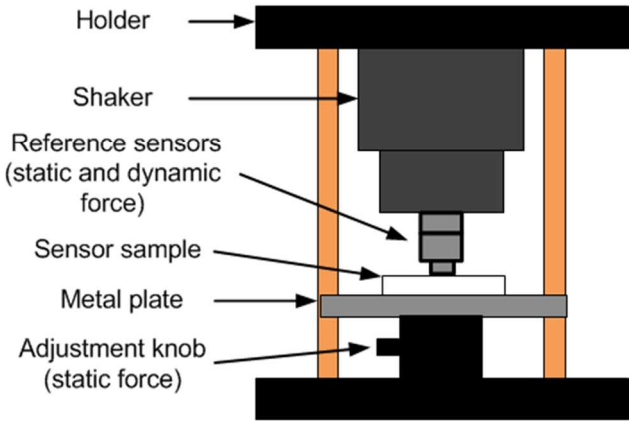

Figure 3. The sensor sensitivity measurement setup.

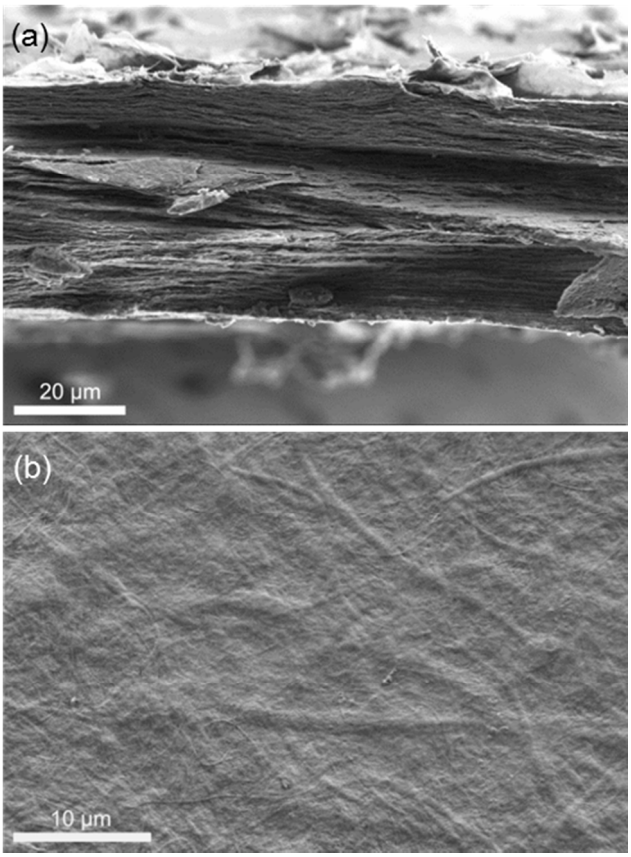

Figure 4. (a) Cross-section and (b) plane view images (SEM) of a CNF film.

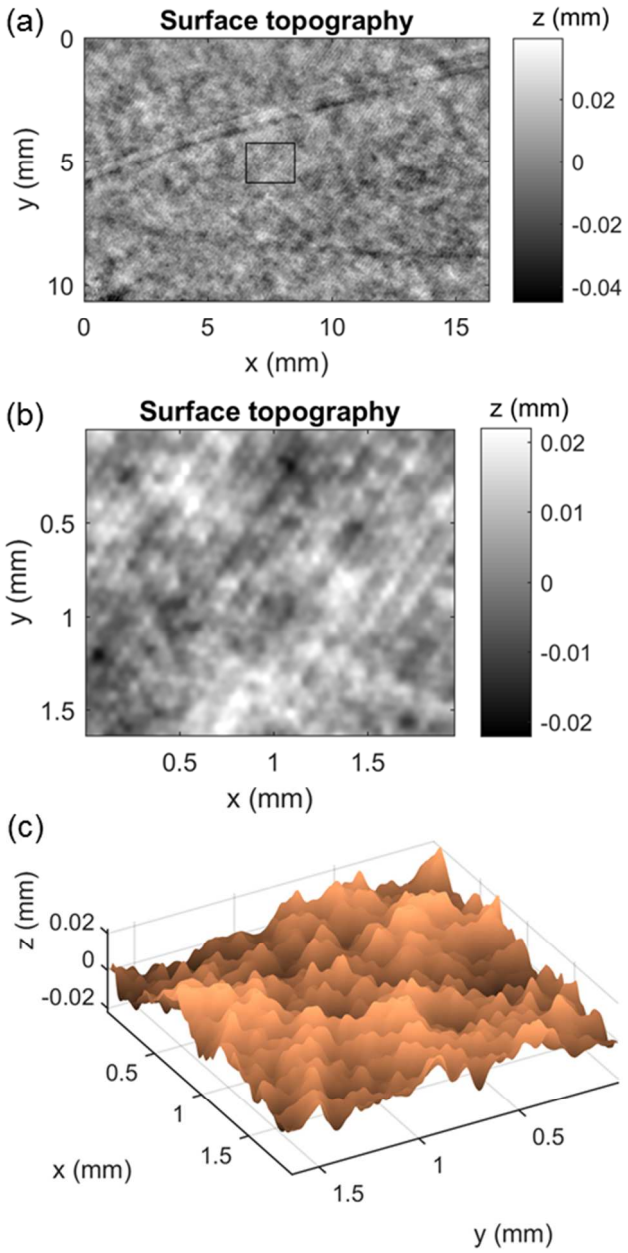

Figure 5. (a) CNF surface topography map and (b) 2D and (c) 3D close-ups (inside the black box in (a)).

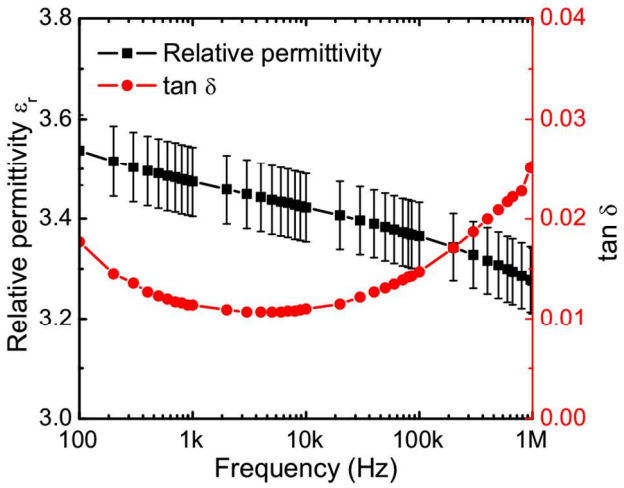

Figure 6. Relative permittivity and loss tangent (tan δ) of CNF film obtained from LCR measurements.

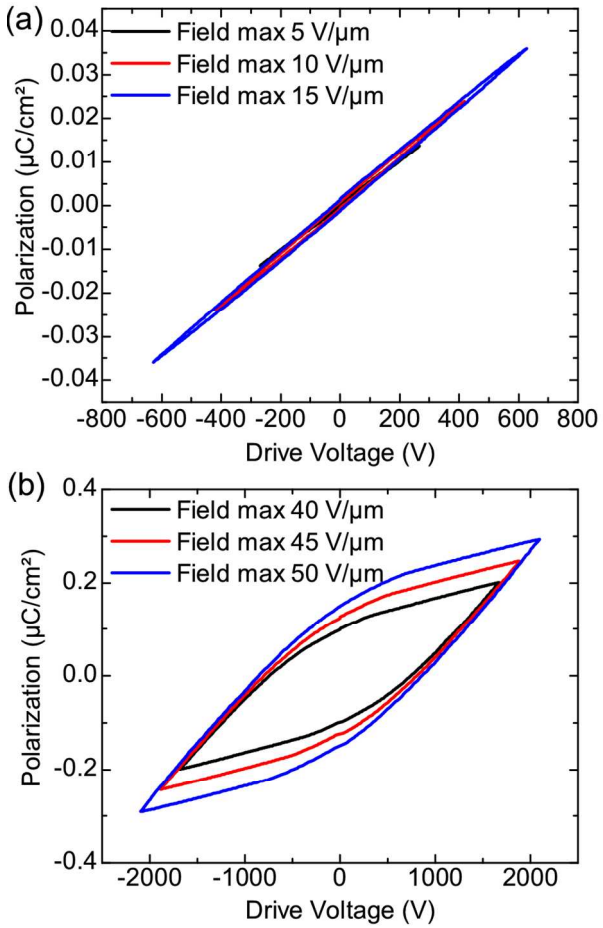

Figure 7. The polarization-voltage hysteresis measurement of CNF (a) at 5-15 V/μm and (b) 40-50 V/μm electric fields at room temperature.

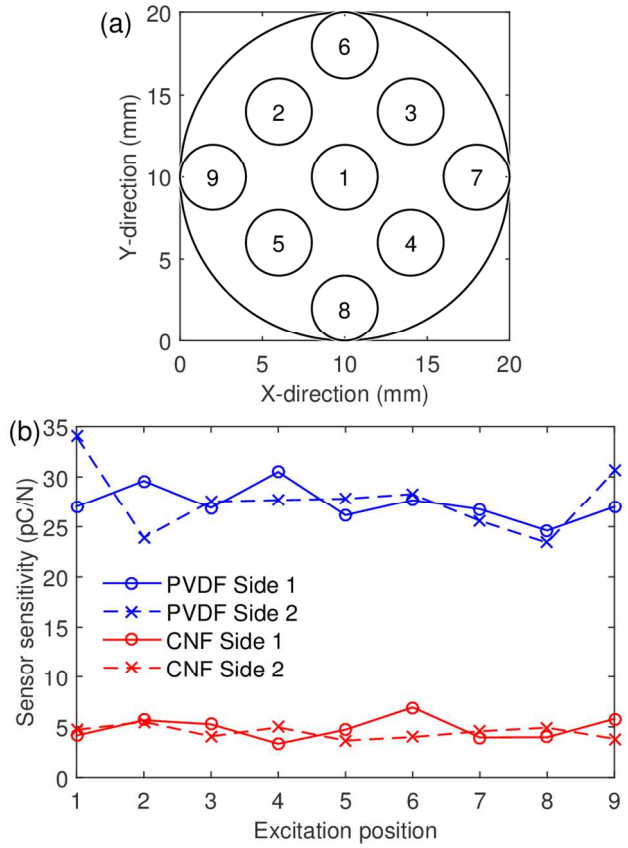

Figure 8. (a) The excitation positions for the sensitivity distribution measurements and (b) the sensor sensitivities as a function of excitation position.

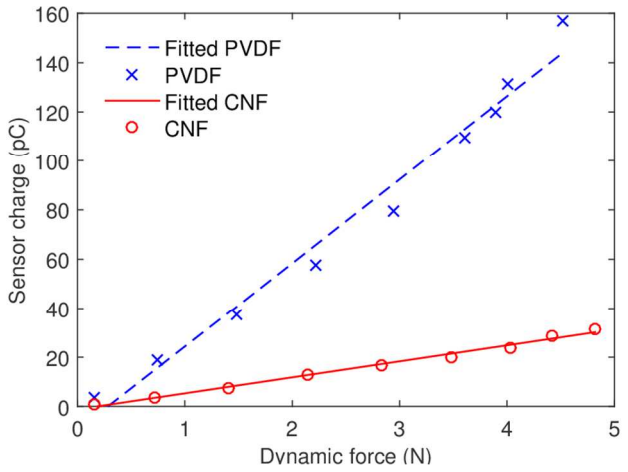

Figure 9. The sensor nonlinearity measurement results for the CNF and reference PVDF sensors.

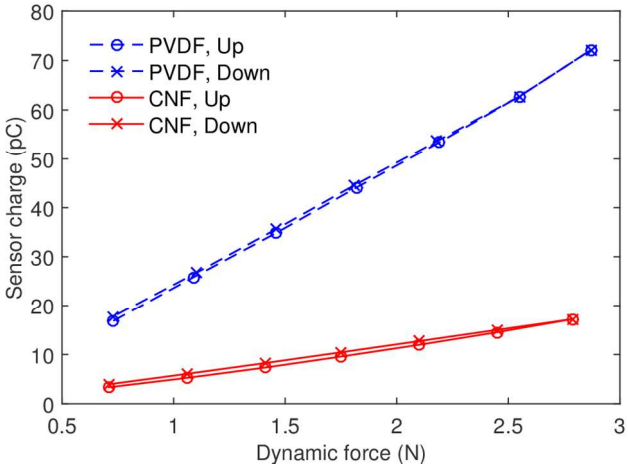

Figure 10. The sensor hysteresis measurement results for the CNF and the reference PVDF sensors.

TABLES.

Table 1. Average force sensitivities for each sensor side.

Sensor name	***Electrode diameter (mm)***	***Sensitivity (pC/N), side 1***	***Sensitivity (pC/N), side 2***	***Sensitivity (pC/N), average***
S1	15	4.7 ± 1.1	5.8 ± 1.6	5.3 ± 1.4
S2	15	5.9 ± 0.9	4.5 ± 0.5	5.2 ± 1.0
S3	15	4.6 ± 0.4	7.4 ± 1.6	6.0 ± 1.9
S4	15	6.1 ± 1.3	6.7 ± 1.2	6.5 ± 1.3
S5	20	4.9 ± 1.1	4.5 ± 0.6	4.7 ± 0.9

AUTHOR INFORMATION

Corresponding Author

*Phone: +358 40 541 5276, Email: sampo.tuukkanen@tut.fi.

Author Contributions

MV has prepared the CNF films. MM has performed the image based analysis for the CNF films. ES has performed the scanning electron microscopy analysis. AP and ST have fabricated the piezoelectric sensors. SR has performed the piezoelectric sensitivity measurements and analyzed the results with ST. TS have performed the dielectric properties and ferroelectric hysteresis measurements and analyzed the results with JJ. SR and ST wrote the most of the manuscript. All authors commented the manuscript and gave their approval to the final version of the manuscript. ‡These authors contributed equally.

Notes

The authors declare no competing financial interest.

ACKNOWLEDGMENT

The authors acknowledge funding from the Academy of Finland (Dec. No. 137669, 258124 and 264743).

REFERENCES

(1) Moon, R. J.; Martini, A.; Nairn, J.; Simonsen, J.; Youngblood, J. Cellulose Nanomaterials Review: Structure, Properties and Nanocomposites. *Chem. Soc. Rev.* **2011**, *40* (7), 3941.

(2) Vuorinen, T.; Zakrzewski, M.; Rajala, S.; Lupo, D.; Vanhala, J.; Palovuori, K.;

Tuukkanen, S. Printable, Transparent, and Flexible Touch Panels Working in Sunlight and Moist Environments. *Adv. Funct. Mater.* **2014**, *24* (40), 6340–6347.

(3) Lehtimäki, S.; Tuukkanen, S.; Pörhönen, J.; Moilanen, P.; Virtanen, J.; Honkanen, M.; Lupo, D. Low-Cost, Solution Processable Carbon Nanotube Supercapacitors and Their Characterization. *Appl. Phys. A* **2014**, *117* (3), 1329–1334.

(4) Rim, Y. S.; Bae, S.-H.; Chen, H.; De Marco, N.; Yang, Y. Recent Progress in Materials and Devices toward Printable and Flexible Sensors. *Adv. Mater.* **2016**.

(5) Isoniemi, T.; Tuukkanen, S.; Cameron, D. C.; Simonen, J.; Toppari, J. J. Measuring Optical Anisotropy in poly(3,4-Ethylene Dioxythiophene):poly(styrene Sulfonate) Films with Added Graphene. *Org. Electron.* **2015**, *25*, 317–323.

(6) Tuukkanen, S.; Lehtimaki, S.; Jahangir, F.; Eskelinen, A.-P.; Lupo, D.; Franssila, S. Printable and Disposable Supercapacitor from Nanocellulose and Carbon Nanotubes. In *Proceedings of the 5th Electronics System-integration Technology Conference (ESTC)*; IEEE, 2014; pp 1–6.

(7) Torvinen, K.; Lehtimäki, S.; Keränen, J. T.; Sievänen, J.; Vartiainen, J.; Hellén, E.; Lupo, D.; Tuukkanen, S. Pigment-Cellulose Nanofibril Composite and Its Application as a Separator-Substrate in Printed Supercapacitors. *Electron. Mater. Lett.* **2015**, *11* (6), 1040–1047.

(8) Lehtimäki, S.; Suominen, M.; Damlin, P.; Tuukkanen, S.; Kvarnström, C.; Lupo, D. Preparation of Supercapacitors on Flexible Substrates with Electrodeposited PEDOT/Graphene Composites. *ACS Appl. Mater. Interfaces* **2015**, *7* (40), 22137–22147.

(9) Fukada, E. Piezoelectricity of Wood. *J. Phys. Soc. Japan* **1955**, *10* (2), 149–154.

(10) Fukada, E. Piezoelectricity as a Fundamental Property of Wood. *Wood Sci. Technol.* **1968**, *2* (4), 299–307.

(11) Harrison, J. S.; Ounaies, Z. Piezoelectric Polymers. In *Encyclopedia of Polymer Science and Technology*; John Wiley & Sons, Inc.: Hoboken, NJ, USA, 2002; Vol. 3.

(12) Csoka, L.; Hoeger, I. C.; Rojas, O. J.; Peszlen, I.; Pawlak, J. J.; Peralta, P. N. Piezoelectric Effect of Cellulose Nanocrystals Thin Films. *ACS Macro Lett.* **2012**, *1* (7), 867–870.

(13) Cheng, H. FlexoElectric Nanobiopolymers (FEPs) Exhibiting Higher Mechanical Strength (7.5 GPa), Modulus (250 GPa), and Energy Transfer Efficiency (75%). *Worldw. Electroact. Polym. (Artificial Muscles) Newsl.* **2008**, *10* (2), 5–7.

(14) Frka-Petesic, B.; Jean, B.; Heux, L. First Experimental Evidence of a Giant Permanent Electric-Dipole Moment in Cellulose Nanocrystals. *EPL (Europhysics Lett.* **2014**, *107* (2), 28006.

(15) Rajala, S.; Vuoriluoto, M.; Rojas, O. J.; Franssila, S.; Tuukkanen, S. Piezoelectric Sensitivity Measurements of Cellulose Nanofibril Sensors. In *Proc. XXI IMEKO World Congr.*; Prague, Czech Republic, 2015; pp 2–6.

(16) Tuukkanen, S.; Rajala, S. A Survey of Printable Piezoelectric Sensors. In *Proc. IEEE SENSORS Conference*; IEEE: Busan, South Korea, 2015; pp 1–4.

(17) Pääkko, M.; Ankerfors, M.; Kosonen, H.; Nykänen, a.; Ahola, S.; Österberg, M.; Ruokolainen, J.; Laine, J.; Larsson, P. T.; Ikkala, O.; Lindström, T. Enzymatic Hydrolysis Combined with Mechanical Shearing and High-Pressure Homogenization for Nanoscale

Cellulose Fibrils and Strong Gels. *Biomacromolecules* **2007**, *8* (6), 1934–1941.

(18) Österberg, M.; Vartiainen, J.; Lucenius, J.; Hippi, U.; Seppälä, J.; Serimaa, R.; Laine, J. A Fast Method to Produce Strong NFC Films as a Platform for Barrier and Functional Materials. *ACS Appl. Mater. Interfaces* **2013**, *5* (11), 4640–4647.

(19) Woodham, R. J. Photometric Method for Detemining Surface Orientation from Multiple Images. *Opt. Eng.* **1980**, *19* (1), 139–144.

(20) Goldman, D. B.; Curless, B.; Hertzmann, A.; Seitz, S. M. Shape and Spatially-Varying BRDFs from Photometric Stereo. *IEEE Trans. Pattern Anal. Mach. Intell.* **2010**, *32* (6), 1060–1071.

(21) Mettänen, M. Measurement of Print Quality: Joint Statistical Analysis of Paper Topography and Print Defects, Tampere University of Technology, 2010.

(22) Sohaib, A.; Farooq, A. R.; Atkinson, G. a; Smith, L. N.; Smith, M. L.; Warr, R. In Vivo Measurement of Skin Microrelief Using Photometric Stereo in the Presence of Interreflections. *J. Opt. Soc. Am. A. Opt. Image Sci. Vis.* **2013**, *30* (3), 278–286.

(23) Frankot, R. T.; Chellappa, R. Method for Enforcing Integrability in Shape From Shading Algorithms. *IEEE Trans. Pattern Anal. Mach. Intell.* **1988**, *10* (4), 439–451.

(24) Harsányi, G. Polymer Films in Sensor Applications: A Review of Present Uses and Future Possibilities. *Sens. Rev.* **2000**, *20* (2), 98–105.

(25) Lang, S. B.; Muensit, S. Review of Some Lesser-Known Applications of Piezoelectric and Pyroelectric Polymers. *Appl. Phys. A Mater. Sci. Process.* **2006**, *85* (2), 125–134.

(26) Rajala, S.; Lekkala, J. Film-Type Sensor Materials PVDF and EMFi in Measurement of Cardiorespiratory Signals a Review. *IEEE Sens. J.* **2012**, *12* (3), 439–446.

(27) Tuukkanen, S.; Julin, T.; Rantanen, V.; Zakrzewski, M.; Moilanen, P.; Lilja, K. E.; Rajala, S. Solution-Processible Electrode Materials for a Heat-Sensitive Piezoelectric Thin-Film Sensor. *Synth. Met.* **2012**, *162* (21-22), 1987–1995.

(28) Kärki, S.; Lekkala, J.; Kuokkanen, H.; Halttunen, J. Development of a Piezoelectric Polymer Film Sensor for Plantar Normal and Shear Stress Measurements. *Sensors Actuators, A Phys.* **2009**, *154* (1), 57–64.

(29) Measurement Specialties Inc. Piezo film sensors, Technical manual http://www.meas-spec.com (accessed May 5, 2014).

(30) S. Kärki, M. Kiiski, M. Mäntysalo, J. L. A PVDF Sensor with Printed Electrodes for Normal and Shear Stress Measurements on Sole. In *Proc. XIX IMEKO World Congr.*; Lisbon, Portugal, 2009; pp 1765–1769.

(31) Tuukkanen, S.; Julin, T.; Rantanen, V.; Zakrzewski, M.; Moilanen, P.; Lupo, D. Low-Temperature Solution Processable Electrodes for Piezoelectric Sensors Applications. *Jpn. J. Appl. Phys.* **2013**, *52* (5S1), 05DA06.

(32) Rajala, S. N. K.; Mettanen, M.; Tuukkanen, S. Structural and Electrical Characterization of Solution-Processed Electrodes for Piezoelectric Polymer Film Sensors. *IEEE Sens. J.* **2016**, *16* (6), 1692–1699.

(33) Rajala, S.; Tuukkanen, S.; Halttunen, J. Characteristics of Piezoelectric Polymer Film Sensors With Solution-Processable Graphene-Based Electrode Materials. *IEEE Sens. J.*

2015, *15* (6), 3102–3109.

(34) Ramadan, K. S.; Sameoto, D.; Evoy, S. A Review of Piezoelectric Polymers as Functional Materials for Electromechanical Transducers. *Smart Mater. Struct.* **2014**, *23* (3), 033001.

(35) Fraden, J. *Handbook of Modern Sensors: Physics, Designs, and Applications, 2nd Ed.*; 2010.

(36) Paajanen, M.; Lekkala, J.; Kirjavainen, K. ElectroMechanical Film (EMFi) — a New Multipurpose Electret Material. *Sensors Actuators A Phys.* **2000**, *84* (1-2), 95–102.

(37) Barna, L., Koivuluoma, M., Hasu, M., Tuppurainen, J. and Värri, A. The Use of Electromechanical Film (EMFi) Sensors in Building a Robust Touch-Sensitive Tablet-like Interface. *IEEE Sens. J.* **2007**, *7* (1), 74–80.

(38) DuPont, DuPont Kapton FPC Polyimide Film, Technical Data Sheet http://www.dupont.com/content/dam/dupont/products-and-services/membranes-and-films/polyimde-films/documents/DEC-Kapton-FPC-datasheet.pdf (accessed Mar 2, 2016).

(39) Perrier, G.; Bergeret, A. Polystyrene-Glass Bead Composites: Maxwell-Wagner-Sillars Relaxations and Percolation. *J. Polym. Sci. Part B Polym. Phys.* **1997**, *35* (9), 1349–1359.

(40) Horiuchi, S.; Tokura, Y. Organic Ferroelectrics. *Nat. Mater.* **2008**, *7* (5), 357–366.

(41) Fukada, E. History and Recent Progress in Piezoelectric Polymers. *IEEE Trans. Ultrason. Ferroelectr. Freq. Control* **2000**, *47* (6), 1277–1290.